

## Bridge structures as sense of displacement criteria in brittle fault zones

J. F. GAMOND

Unité Associée au CNRS N°. 733, Institut de Recherches Interdisciplinaires de Géologie et de Mécanique,  
 B.P. 68, 38402 St Martin d'Hères Cédex, France

(Received 27 June 1986; accepted in revised form 13 March 1987)

**Abstract**—Fault zones often occur as arrays of en-échelon fractures. There are two main types of en-échelon patterns, involving right- or left-stepping fractures. In such arrays, first-generation fractures define compressive or tensile bridges. The structural features of such natural bridges, at any scale, can be used as criteria to determine the sense of displacement. Small compressive bridges provide criteria based on the increase in linear density of solution seams related to the degree of asymmetry of the fault trace, and to the sequence of formation of the different types of en-échelon fractures. The criteria deduced from large compressive bridges involve upward displacement of the material by folds and hill or mountain ranges, asymmetry of the fault profile and relative chronology of the segments. Tensile bridges yield criteria based upon vein fillings, asymmetry and relative chronology. In large-scale structures some pull-apart basins are shown to be bounded by normal faults parallel to, but outside, the strike-slip segments. From a comparison of analytical models with well-known large-scale fault zones, a new criterion can be proposed. In fault zones formed through coalescence of en-échelon fractures the bridging segments are wide if facing leeward of the bulk movement sense, and narrow if forward-facing.

### INTRODUCTION

IT IS COMMONLY observed, at all scales, that faults are not ideal planar surfaces but rather occur as arrays of second-order en-échelon fractures which combine and anastomose. These fractures belong to several classical types which are defined by their attitude relative to the general direction and sense of the fault. Two main types of en-échelon patterns can be distinguished, as shown in Fig. 1: right-stepping fractures on left-lateral shear, or left-stepping fractures on right-lateral shear (RS/LL or LS/RL, respectively, Fig. 1a), and left-stepping fractures on left-lateral shear or right-stepping fractures on right-lateral shear (LS/LL or RS/RL, respectively, Fig. 1b). The observations made by many authors in natural mesofaults (Hancock 1972, 1985, Beach 1975, Robert & Vialon 1976, Gamond 1983, 1985, Petit *et al.* 1983) as well as in physical models (Morgenstern & Tchalenko

1967, Bartlett *et al.* 1981) suggest that the different types of en-échelon fractures do not form at the same time but according to a particular sequence. For a left-lateral fault zone, this sequence consists of a first-generation array of right-stepping fractures bounding 'bridges' of intact rock which are later cut by second-generation left-stepping shear fractures. Even before failure occurs in the bridges, the general displacement on the fault zone causes the first-generation fractures to slip in the same sense (this sliding sometimes even combines with the opening of en-échelon veins as shown by Hancock 1985, fig. 11d). Such an evolution creates compression forces in the bridges (C, in Fig. 1a) which continue acting after the second-generation fractures have formed. Large-scale structures similar to these compressive bridges are described as 'restraining bends' (Crowell 1974, Woodcock & Fischer 1986) or as 'antidilational jogs' (Sibson 1986). The sequence of fractures producing

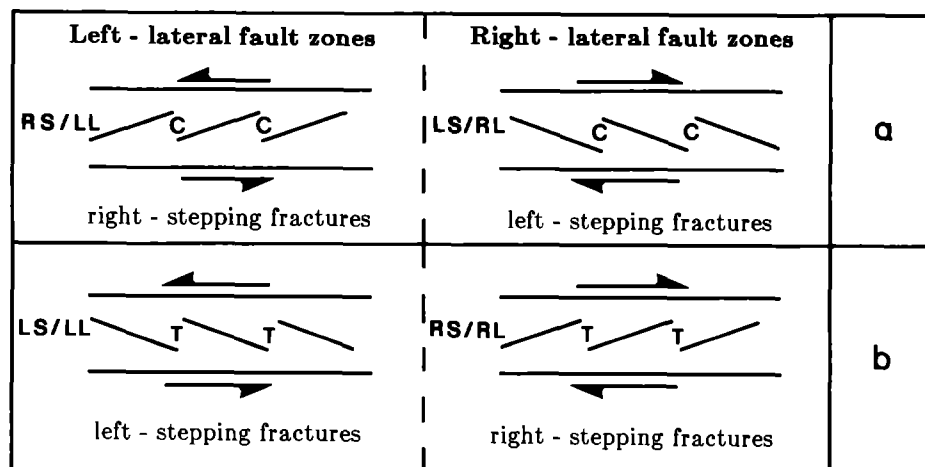


Fig. 1. The two main types of en-échelon patterns for both left- and right-lateral fault zones. (a) Patterns providing compressive bridges and (b) tensile bridges.

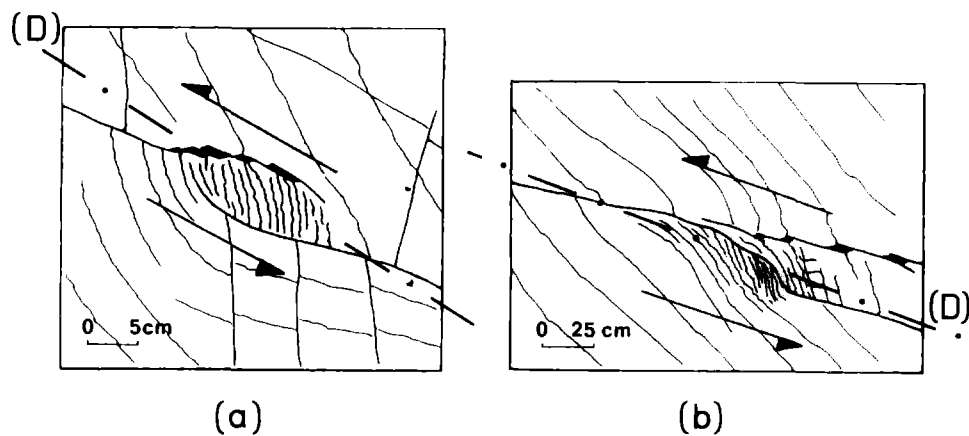


Fig. 2. Examples of natural compressive bridges in Languedoc limestones. The increase in density of the stylolitic surfaces indicates a higher stress level in the bridge and the change in their direction shows that the maximum principal stress is reoriented with respect to its far-field direction. (a) Before fracturing of the bridge. (b) A more advanced stage, after fracturing of the bridge by a second-generation shear fracture.

compressive bridges is often interpreted in terms of brittle or pseudo-plastic rupture and is related to the stress orientation which is assumed to exist in a shear zone developing in a homogeneous stress field. According to this interpretation, the LS/LL (or RS/RL) fractures could only form as second-generation shear fractures, their attitude resulting from the stress reorientation in the bridges (Morgenstern & Tchalenko 1967, Naylor *et al.* 1986).

Although no interpretation in terms of stress can be proposed concerning the genesis of LS/LL (or RS/RL) fractures, they also happen to produce first-generation arrays, as shown by many field examples. In these cases, when the displacement on the fault zone increases, the bridges undergo extension (T, in Fig. 1b). These tensile bridges are likely to break later by RS/LL (or LS/RL) second-generation fractures. Large-scale structures similar to the tensile bridges are described as 'releasing bends' or as 'dilatational jogs'.

The aim of this paper is to use the characteristic features of bridge structures, at any scale, as criteria for determining the sense of displacement. First, field examples of compressive and tensile bridges will be described. The stress level variations across each type of bridge will be considered from theoretical models of other authors, and the influence of the stress level on the fault zone structure studied by means of analogue clay models. The results are used to propose a new shear criterion for faults based on the relative width of consecutive segments in large fault zones.

## CHARACTERISTICS OF NATURAL COMPRESSIVE BRIDGES

### *Small structures*

In Languedoc (near Montpellier), many limestone beds in homogeneous areas free of mesofaults contain stylolitic columns, normal to the planar stylolitic seams. These planar seams are virtually parallel, a few centimet-

ers apart. This regular pattern indicates shortening of constant orientation, parallel to the columns, which can be considered as the direction of regional  $\sigma_1$ . Mesofaults are found on the surface of these beds in an early stage of development consisting of arrays of en-échelon first-generation fractures at an angle of 10–15° to the general discontinuity direction (D). The offsets of the fractures define compressive bridges. The stylolitic seams in these bridges become closer and more numerous which is indicative of an increase in pressure solution and stress level. In these areas the seams also change direction, with the columns keeping normal to them. This means that the maximum principal stress is reoriented clockwise for right-stepping fractures on a left-lateral fault zone. According to Xiahoan (1983) the stylolitic seams in the bridges in Fig. 2 (a & b) develop between non-overlapping en-échelon primary fractures. It is only at a more advanced stage that a second-generation fracture links up with the pre-existing ones (Fig. 2b).

The Grandes Rousses gneisses display fault zones composed of two sets of en-échelon fractures, one right-stepping, the other left-stepping, (Fig. 3). These fractures are more or less symmetrical with respect to the general direction (D) of the left-lateral shear plane. In view of their angles, the right-stepping ones are interpreted as R fractures and the left-stepping ones as P fractures. Sliding on the P surfaces has caused the R fractures to open into prismatic gaps (dominoes) which are now filled with quartz. Although this opening appears to be a tensile bridge, it was shown (Gamond 1983) that the R fractures form first and that there are compressive bridges between their adjacent tips, subsequently broken by second-generation P fractures. In these gneisses, the magnitude of displacements parallel to (D) can be measured by the offset of leucocratic marker layers and by the domino openings. The  $d'$  value of the domino opening is lower than the displacement  $d$  on the sliding P fractures:  $d' < d$  (Fig. 3).

A possible interpretation of this phenomenon can be proposed through a simple geometrical plane-strain model in which volume loss is assumed to combine with

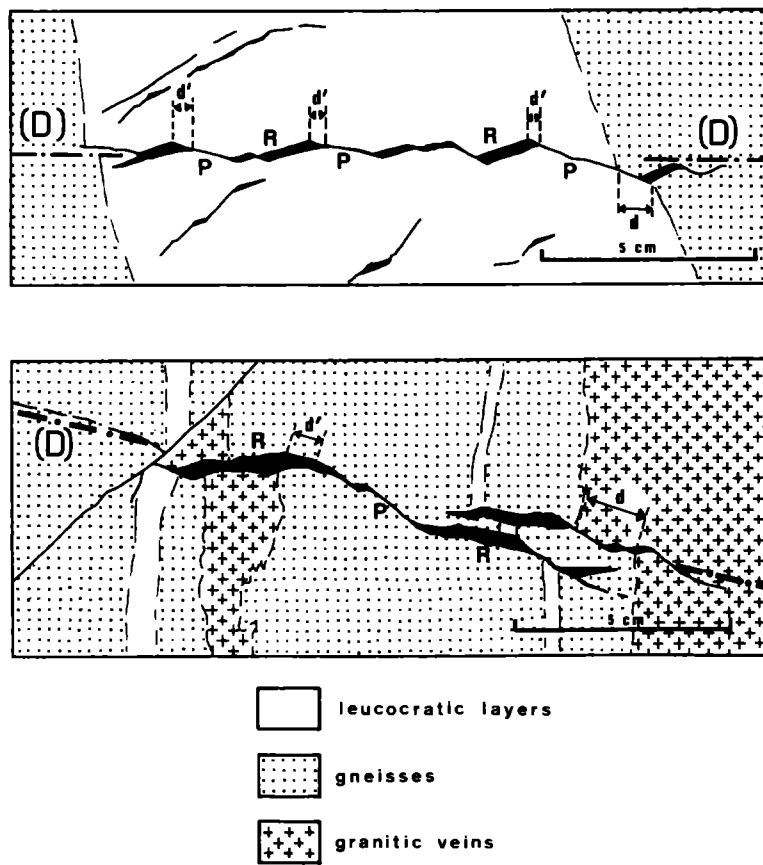


Fig. 3. Evidence for pressure-solution phenomena along second-generation P fractures on small fault zones in the Grandes Rousses gneisses. For explanation see text.

sliding on the second-generation fractures (Fig. 4). Part of a left-lateral discontinuity (LLD) is considered to have two second-order fractures: ( $RS_1$ ) a first-generation crack and ( $LS_2$ ) a second-generation one, each assumed to be part of an array of en-échelon cracks which define (LLD).  $RS_1$  and  $LS_2$  link at A and separate an upper block (U) from a lower block (L). Before any sliding occurs (Fig. 4a) the marker on the right has no offset. In Fig. 4(b), only the sliding governed by  $LS_2$  and the opening of the gaps in the general movement on (LLD), are sketched. The displacement component parallel to (LLD) is  $d$ , whether it is measured with the marker or with the  $A_U-A_L$  offset.

In natural cases, if sliding is associated with volume loss in the material, both phenomena probably combine in each incremental displacement on (LLD). Figure 4(c) shows the area corresponding to the volume to be lost by moving one block into the other over a distance ( $n$ ), perpendicular to (LLD), while sliding (sl) occurs on  $RS_1$ . Point  $A_L$  thus vanishes and the new intersection  $RS_1/LS_2$  becomes  $A'_L$ . The picture resulting from superimposed sliding and volume loss is given in Fig. 4(d). The displacement value  $d$  measured parallel to (LLD) with the marker offset is not modified with respect to Fig. 4(a)–(c). However, owing to volume loss, if it is measured between  $A_U$  and  $A'_L$ , then  $d' < d$ . The actual displacement vector (R) between block (U) and block (L) is the sum of (sl) and ( $n$ ) and is slightly oblique to (LLD). Depending on the relative lengths of (sl) and

( $n$ ), (R) could correspond to diverging, converging or parallel displacement of the two blocks with respect to LLD.

#### Large structures

Compressive bridges are also found in large fault zones.

In South California the right-lateral NW-striking Coyote Creek fault displaced by the 1968 Borrego Mountain Earthquake, shows two 10 km long left-stepping segments (Fig. 5). Within the bridge, in the Ocotillo Badlands region, a topographic relief rising 200 m above the surrounding desert corresponds to sedimentary strata warped into sigmoidal folds (Segall & Pollard 1980). Since the bridge is not broken by a second-generation segment it can be inferred that this case is an early stage of a fault zone with small displacement. Given the small angle ( $10-15^\circ$ ) between the general trend of the fault zone (D on Fig. 5) and the individual segments, these segments have an attitude similar to that of R fractures in a mesofault zone. Since each individual strike-slip segment is much longer than the bridge area, the resulting structure is asymmetric with respect to (D).

The large left-lateral Dead Sea crustal fault has two N-striking segments: the Jordan Fault in Israel and the Orontes Fault in Syria (Fig. 6a). The strike-slip displacement on these fault segments ranges from 70 km (Orontes segment) to 100 km (Jordan segment). The

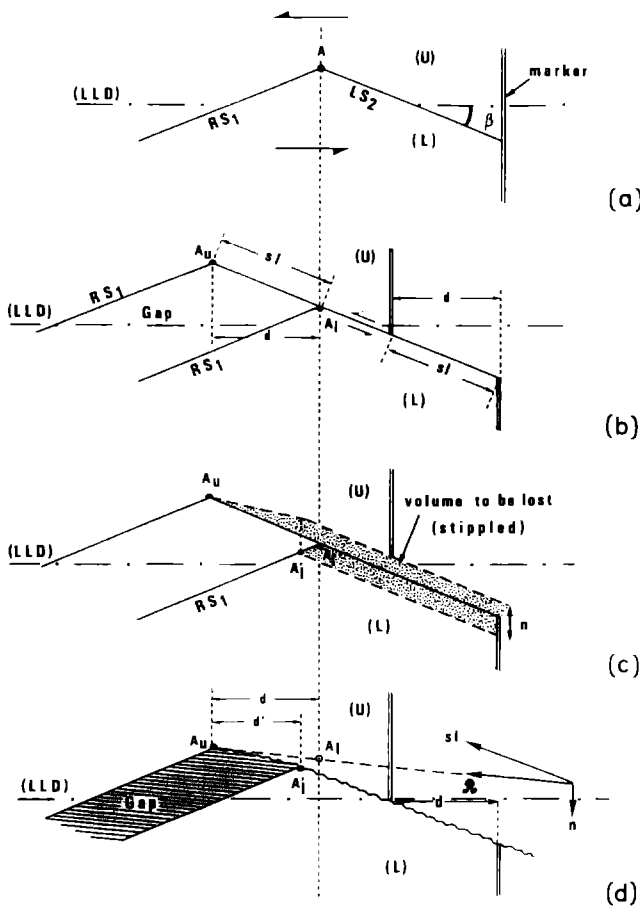


Fig. 4. Geometrical decomposition of sliding on a plane oblique to main displacement  $D$ , combined with pressure solution. (a) Initial state. (b) Sliding component only. (c) Limits of the volume to be dissolved under transpression (stippled). (d) Finite geometry and resultant displacement vector. See text for details.

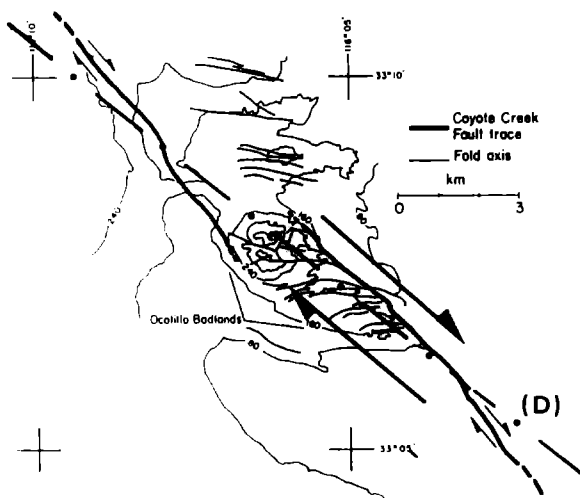


Fig. 5. The Ocotillo Badlands area, a compressive bridge between two left-stepping segments corresponding to a topographic relief formed by en-échelon sigmoidal folds (slightly modified from Segall & Pollard 1980).

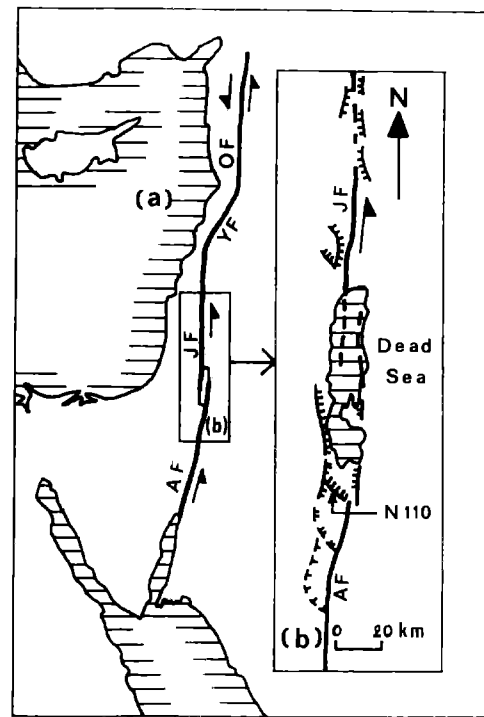


Fig. 6. General setting of the Dead Sea Fault. (a) The Yammuné Fault (YF) appears in the compressive bridge between the two N-trending right-stepping segments of the Jordan Fault (JF) and Orontes Fault (OF). (b) Between the left-stepping Jordan fault and Arava Fault (AF), the Dead Sea is assumed to be a rhomb graben through transverse N110° normal faults.

compressive bridge between these two segments is assumed to reflect the 25 km crustal shortening (Freund *et al.* 1970) corresponding to the movement of the Levantine plate into the Arabian plate which elevated the N30°-trending Lebanese ranges to 2800–3000 m. Such deformation is equivalent to 'simple transpression' as defined by Harland (1971) and Sanderson & Marchini (1984) and is also similar to Woodcock & Fischer's (1986) 'restraining bends' in strike-slip duplexes. A detailed analysis of this deformation is given by Hancock & Atiya (1979). The shortening is achieved through folds which were subjected to an anticlockwise rotation to N30° during the late Paleogene, and conjugate strike-slip faults corresponding to an axial elongation. In the western range the folds are outward-facing box-folds associated with ESE-dipping reverse faults, contrary to the eastern range where the folds are inclined towards the Arabian plate and parallel to WNW-dipping reverse faults. This flower-structure shows that the material is ejected towards the stress-free surface. In the middle of and parallel to the fold belt, the narrow Yammuné fault zone (2 km wide) appeared during the Neogene period and has a 7 km left-lateral displacement. This late-stage event proves to be compressional too, since abundant stylolitic seams have developed parallel to, and in the vicinity of, the fault.

Regardless of the size of the faults, compressive bridges are therefore subject to a decrease in area. In small structures where the fault zone develops entirely inside homogeneous rock, this decrease in area occurs as a volume loss accommodated either by pressure solution

along numerous stylolitic seams or by solution and/or compaction along a second-generation shear fracture developing across the bridge. In large wrench-faults the bridge area is decreased by driving inhomogeneous material (layered rocks for instance) up towards the stress-free surface through the formation of pressure ridges, folds and flower-structure patterns. When the displacement increases, both in small and in large structures, a second-generation shear zone has to propagate through the bridge.

### CHARACTERISTICS OF NATURAL TENSILE BRIDGES

#### *Small structures*

In many tensile bridges of left-lateral faults (Petit 1976, Raynaud 1979, Xiahoan 1983, Gamond 1985) the left-stepping individual fractures are shear fractures at angles of about  $15^\circ$  to the general direction (D). These fractures thus have the same attitude as P fractures (Fig. 7) and will be called P' fractures. The second type of fracture, which opens when slip occurs on the first ones, makes various angles with D (mean value  $40^\circ$ ) thereby giving the fault an asymmetric profile. The chronology assumed for these bridges may be proved by several indicators. First, the angles between (D) and P' fractures are fairly constant, contrary to the right-stepping fractures whose orientations are not so regular. The left-stepping fractures should therefore correspond to primary ruptures in a medium with little disturbance of the principal stresses directions. In addition, the left-stepping fractures often overlap when the right-stepping fractures are located within the overlapped area. These H-shaped patterns, where the younger traces abut the older ones (Hancock 1985), give proof of the secondary extension of the bridges. The right-stepping fractures may thus be assumed to be second-generation tension gashes.

Stylolitic seams are often observed near small faults with tensile bridges in carbonates, but they do not occupy specific sites since they develop without preference near right- or left-stepping elementary fractures, without noticeable reorientation. In such cases diffuse pressure solution occurs, with no indication that it combines with slip on P' fractures, contrary to the compressive bridges described above.

#### *Large structures*

Large tensile bridges are generally rhomb grabens or pull-apart basins. Such systems can be seen along the Jordan left-lateral fault (from the Red Sea to Lebanon). This crustal discontinuity consists of left-stepping en-échelon segments with their bridges broken by pull-aparts such as the Gulf of Eilat and the Dead Sea. The latter develops between two N-striking segments 15 km apart (Fig. 6b). The  $N110^\circ$  normal faults which are formed between these segments allow the two blocks to separate and to slip. Once again the fault profile is very asymmetrical. The topographic depression, 400 m below the level of the Mediterranean Sea, is bounded by large throw normal faults parallel to, but outside, the strike-slip segments.

The latter characteristic can also be observed on the Glynnwye depression in the Hope right-lateral fault zone (New Zealand) (Fig. 8a). The right-lateral displacement measured from the offset of a moraine is 300 m; the separation of the en-échelon strike-slip segments is 200 m. These should therefore be the dimensions of the theoretical basin resulting from the displacement of the two blocks. In fact, normal fault scarps not only parallel to the tensile fractures (WNW-ESE) but also to the strike-slip fractures, give rise to a topographic depression, 900 m long and 500 m wide. Clayton (1966) shows that the adjacent tips of the strike-slip segments converge downdip and suggests, as do Segall & Pollard (1980), that these surfaces join together at depth to form a single plane. The depressions likely to develop within

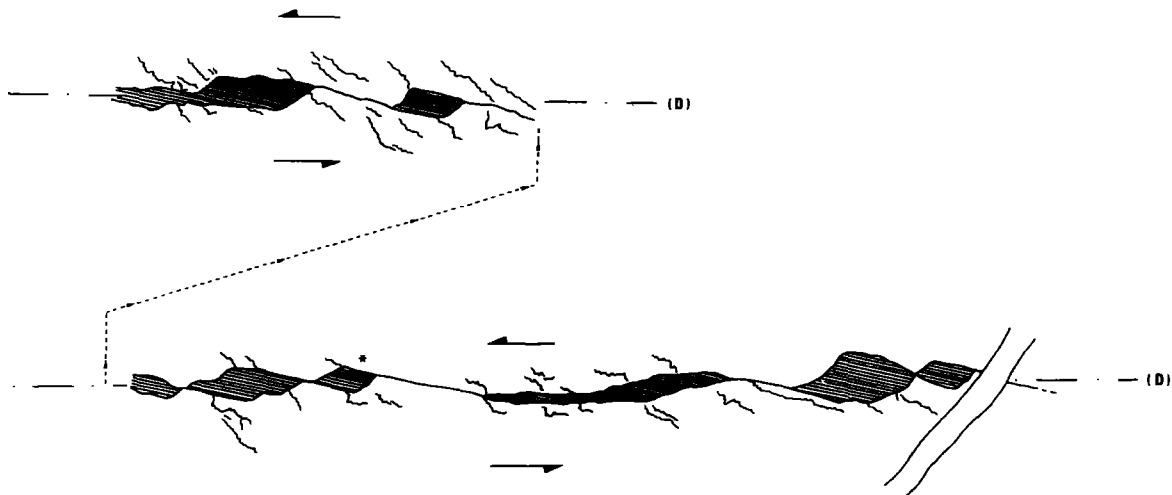


Fig. 7. Calcite dominoes opening in tensile bridges of a left-lateral discontinuity (D). The discontinuity is achieved through an association of P' left-stepping first-generation fractures making angles of  $12\text{--}14^\circ$  with (D), and right-stepping second-generation tension fractures [at  $45\text{--}50^\circ$  to (D)].

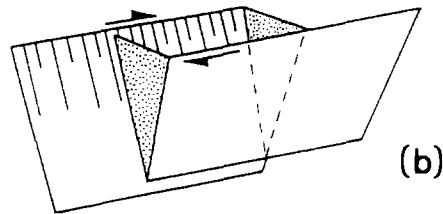
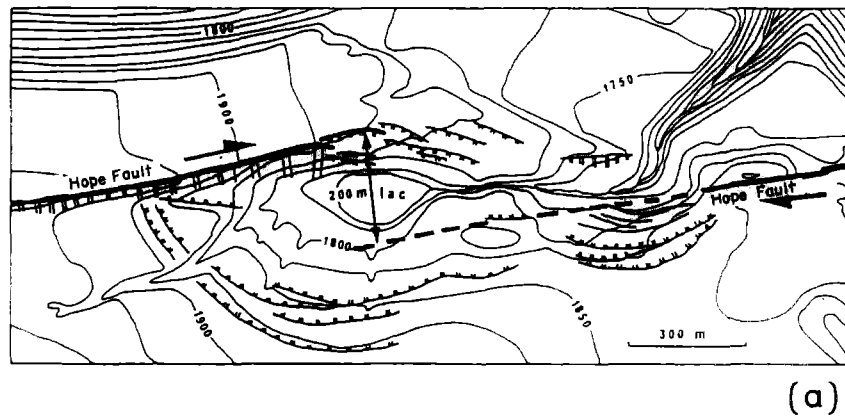


Fig. 8(a). Evidence for normal faults parallel to the right-stepping fractures of the Hope Fault, New Zealand. These normal faults determine a topographic depression wider than the 200 m separation between the wrench segments (modified from Clayton 1966). (b) Theoretical wedge-shaped basin opened by sliding on echelon fractures converging at depth.

tensile bridges should therefore theoretically be wedge-shaped (Fig. 8b) with only two sides corresponding to normal faults.

However, the above field examples show that these basins may be bounded by normal faults parallel to the strike-slip direction, and covering a wider zone than the distance separating the wrench segments. This can be interpreted as a consequence of the collapse of the surrounding material into the wedge-shaped basin as soon as it opens.

## RELATIONSHIPS BETWEEN STRESS LEVEL AND TYPE OF BRIDGE

### *Mathematical models of bridges*

Several mathematical models of these two main types of bridge have been constructed, taking as a basic hypothesis that the material is already broken by an array of left-stepping or right-stepping en-échelon fractures (Segall & Pollard 1980, Xiahaoan 1983). Assuming

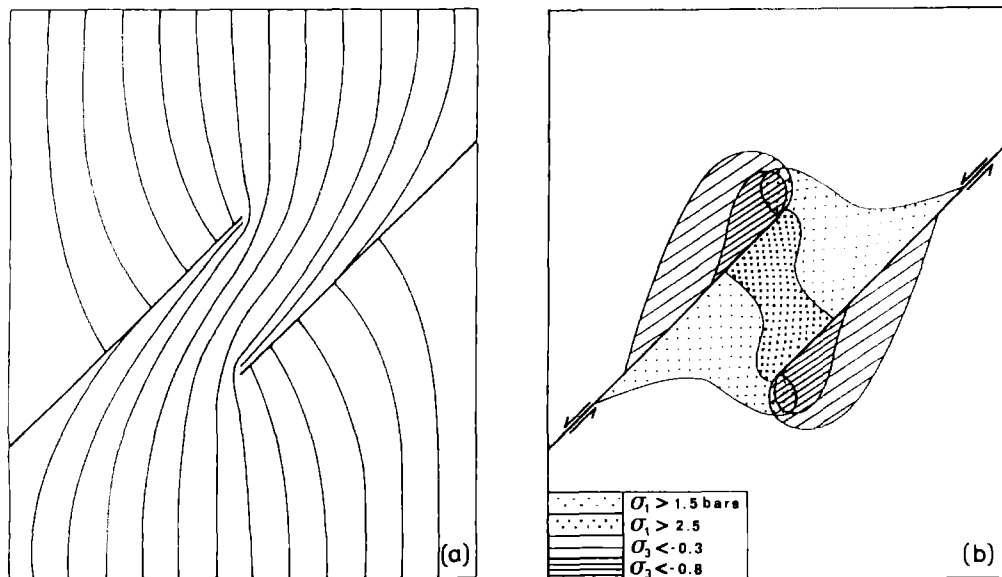


Fig. 9. Mathematical model of a compressive bridge (after Xiahaoan 1983). (a) Reorientation of  $\sigma_1$  trajectories. (b) Modification of  $\sigma_1$  with respect to its far-field value ( $1 \times 10^{-1}$  MPa).

linear elastic behaviour, the calculations give the directions and values of the principal stresses inside and outside the bridge and the potential directions of tensile and shear fractures likely to form in the bridge.

The results obtained by different authors are very similar. In the compressive bridges (Fig. 9) the mean stress and the maximum principal stress increase significantly. In addition, sliding on pre-existing fractures is inhibited by the increase in normal stress and the decrease in shear stress. In small structures, these modifications promote an increase in pressure solution in the bridge and provide a higher density of stylolitic surfaces. In large structures, the increase in stress level gives rise to pressure ridges, folds and ranges.

The models also show stress reorientation. In a compressive bridge on a left-lateral fault,  $\sigma_1$  undergoes a clockwise rotation. Consequently, when the bridge breaks, a shear fracture making an angle of  $(\pi/4 - \phi/2)$  with the new  $\sigma_1$  direction forms (where  $\phi$  is the angle of internal friction), corresponding to the second-generation fractures which propagate through the compressive bridges.

In the tensile bridges (Fig. 10), the previously described phenomena are reversed; i.e. the stress level decreases and slip on pre-existing fractures becomes easier. In the bridges,  $\sigma_1$  is subject to anticlockwise reorientation. Its new direction is similar to that of the second-generation fractures whose opening gives rise to dominoes and rhomb grabens. These fractures are then parallel to the major principal stress and can be considered as tensile fractures. They indicate a change to a more brittle behaviour, entirely consistent with the decrease in the stress level.

When comparing natural and theoretical features, the basic hypotheses of the mathematical models seem realistic. In a medium subjected to a quite homogeneous

stress state from the outset, a fault zone is therefore likely to occur through first-generation en-échelon fractures. While these events are taking place, several parameters remain unchanged: these are the slip rate of the blocks on each side of the fault, the fluid content of the material, and its temperature. In contrast, the variation in stress level with respect to initial values in the bridges is likely to lead to local modifications of the behaviour of the material and subsequently of the features of the fracture zones developing there (as reflected by the second-generation shear fractures in compressive bridges and the tensile fractures in tensile bridges).

### STRESS LEVEL AND FAULT ZONE WIDTH IN MODELS

In order to take into account the effect of stress level on the structure and fracturing of the bridges, analogue models of fault zones were deformed under direct shear conditions. The displacement rate of the box was 1 mm/min, corresponding to undrained tests. The samples measure  $25 \times 15 \times 15$  cm. The material chosen is a homogeneous natural clay, with 22% water content, overconsolidated to 1.4 MPa. These characteristics combined with the low percentage of clay minerals (35%) give this material an adequate stiffness for primary fractures to form when running shear tests, and a behaviour similar to that of a rock, as shown by its parabolic Mohr envelope. The different stress levels are obtained by varying the vertical normal stress applied on the upper surface of the sample.

Several previous direct shear models (Gamond & Giraud 1982, Gamond 1983) showed that the zone of discontinuity imposed by the apparatus is composed of first-generation fractures of the R type joined by second-

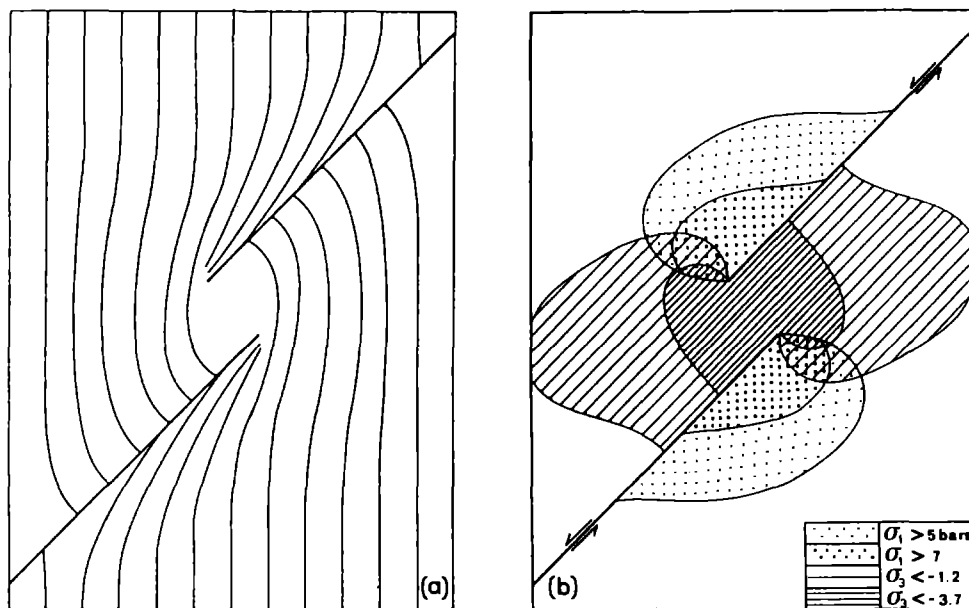


Fig. 10. Mathematical model of a tensile bridge (after Xiaohan 1983). (a) Reorientation of  $\sigma_1$  trajectories. (b) Modifications of  $\sigma_1$  with respect to its far-field value ( $4 \times 10^{-1}$  MPa).

generation P fractures. This relative chronology is consistent with the mechanical interpretation of Morgenstern & Tchalenko (1967). In the three models described below, a similar fracture history was observed, although the illustrations in Fig. 11 show fully developed shear lenses.

In model 1 (Fig. 11a) the vertical stress normal to the fracture zone ( $\sigma_n$ ) is zero. A few R and P fractures, 10 cm long, coalesced to form a zone about 4.5 cm wide. In model 2 ( $\sigma_n = 3 \times 10^{-1}$  MPa) the elementary fractures increased in number but their individual size decreased (Fig. 11b). The fracture zone reached 2 cm in width.

This trend is confirmed in the third model (Fig. 11c) ( $\sigma_n = 7 \times 10^{-1}$  MPa), where even more numerous and short fractures define a zone with width reduced to 1.5 cm.

It seems therefore that the increase in the stress normal to the discontinuity (which is equivalent to an increase of the rupture stress level) tends to increase the number of fractures, to decrease their length, and, the most important point, to reduce the width of the fracture zone. However, Naylor *et al.*, (1986) show that on pre-stressed sandbox models sheared over a basement discontinuity, the fault zone is wider when the horizontal maximum principal stress  $\sigma_1$  is normal to the fault than when it is parallel. Apart from the difference in the materials, my clay models should not be compared with the above models which were not designed to test the stress level effect, nor can they be compared with the models of Hempton & Neher (1986) who studied fractures forming in a clay cake above a tensile bridge pre-cut in a basal plate.

At a given time in the sequence of events of fault zone development, there is a stage where no discontinuity exists in the bridges between first-generation fractures in

the array. The comparison between the mathematical models and certain natural faults indicates significant modification of the stress level in the bridges with respect to that exerted on the previous échelon array. Therefore, if the fault zone width is governed by the change in stress level as indicated by the analogue models, the width of the rupture zones likely to be created through the bridges must be different from that of the first-generation segments. In order to verify if this hypothesis applies to field examples, data on well-known previously described strike-slip faults are re-examined.

### APPLICATION TO FIELD EXAMPLES

The Dasht-e-Bayaz fault (Tchalenko & Ambraseys 1970) which resulted from the 1968 earthquake, affects Quaternary sediments over a distance of 25 km, with a left-lateral displacement of about 4.5 m. It mostly consists of E-W-trending segments about 100 m wide, formed through second-order en-échelon R and P shears. The fault zone includes two bridges, one compressive (Fig. 12a), the other tensile (Fig. 12b). In the compressive bridge, where the stress level is assumed to increase, the width of the N115° fracture zone, also composed of elementary R and P shears, does not exceed 10 m. In the tensile bridge, where a decrease in stress level is forecast by the mathematical models, the N60° fracture zone, combining tensile fractures and conjugate shears, is 1500 m wide.

As a second example the left-lateral crustal discontinuity of the Dead Sea is reconsidered (Fig. 6). In this structure, the transpressive bridge corresponding to the Lebanese ranges is cut longitudinally by the 150 km long N30° Yammuné Fault which is never more than 2 km

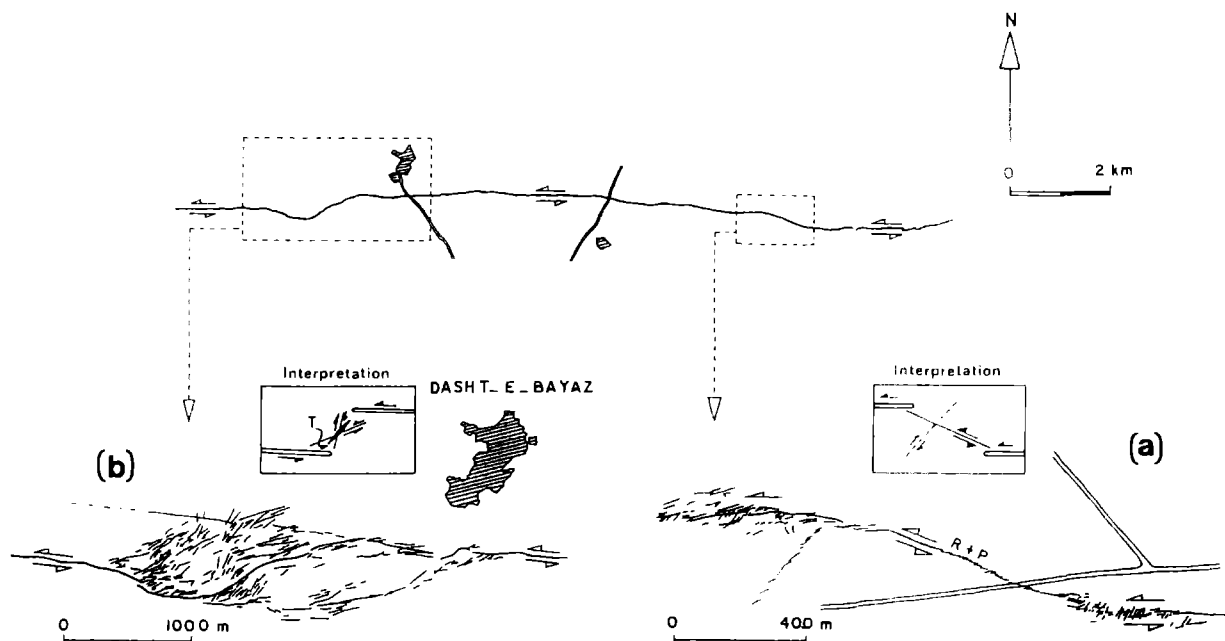


Fig. 12. Evidence of variation in width of the segments of the Dasht-e-Bayaz Fault. (a) In the compressive bridge, between the N90° right-stepping segments, a much narrower N115° fracture zone develops. (b) In the tensile bridge, between two N90° left-stepping segments, a much wider fracture zone develops (modified from Tchalenko & Ambraseys 1970).



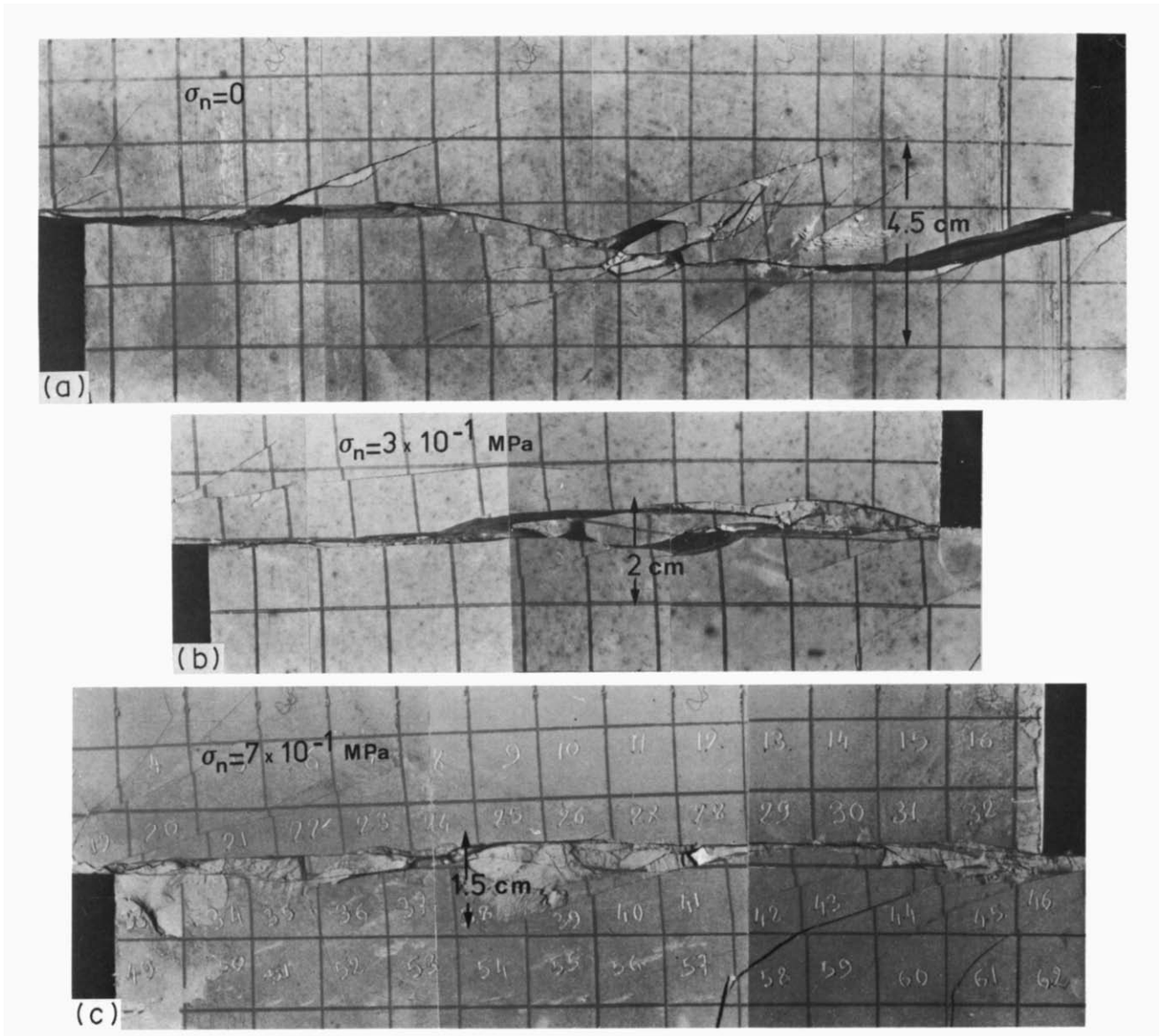


Fig. 11. Analogue clay models. (a) Model 1 under zero normal stress. The discontinuity zone, composed of R- and P-type primary fractures, is 4.5 cm wide. (b) Model 2 with a stress normal to the discontinuity of  $3 \times 10^{-1}$  MPa. The fracture zone is 2 cm wide. (c) Model 3 with a stress normal to the discontinuity of  $7 \times 10^{-1}$  MPa. The width of the zone is reduced to 1.5 cm.





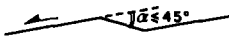

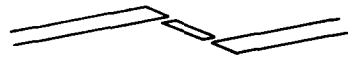

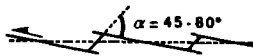



Compressive Bridges *		
	Characteristics	Structural features
small structures	Symmetry, openings and sequence of fractures	
	Asymmetry and pressure solution	
large structures	Asymmetry and angular relationships	
	Asymmetry and shortening	
	Relative width of the segments	
Tensile Bridges *		
small and large structures	Asymmetry and openings	
	Asymmetry and angular relationships	
	Asymmetry, sequence of fractures and openings	
large structures	Asymmetry and normal faults	
	Relative width of the segments	

Fig. 13. A summary of some structural features of compressive and tensile bridges, at various scales, used as criteria for determining the sense of movement on a fault.

wide. On the other hand, the N-trending segments (Jordan Fault and Orontes Fault) are composed of elementary fractures making a zone up to 20 km wide (Hancock & Atiya 1979, Garfunkel *et al.* 1981, Figs. 5 and 6).

Although these two large structures are very different in size (25 km vs 600 km) and displacement (4.5 m vs 100 km), it seems that the segment widths verify the trend shown by the models.

This property is proposed as a new criterion to be used for determining the sense of movement in large fault zones including segments joined by bridges. This criterion is summarized on Fig. 13. It should be emphasised that for any segment, only the width of the fracture zone needs to be taken into account.

### SENSE OF DISPLACEMENT CRITERIA—CONCLUSIONS

From the analysis of brittle fault zones with first-generation en-échelon segments, two main types of bridges, compressive and tensile, can be identified at very different scales. The structural features of these bridges are interpreted by means of mathematical and analogue models in terms of changes in material behaviour, and provide some simple criteria for determining the sense of displacement.

(1) Tensile bridges between en-échelon fractures are indicated by dominoes on the small scale, and rhomb grabens or pull-apart basins at the large scale. The occurrence of normal faults occupying a wider zone than

the separation of the en-échelon segments provides a further indicator to identify these basins.

(2) Compressive bridges exhibit shortening accommodated by pressure solution in small structures, and pressure ridges, folds and even hill or mountain ranges, in large structures. Second-generation shear fractures developing through the bridges generally connect the first generation segments.

(3) The asymmetry of the fault profile, and the angle between the en-échelon fractures and the bridge fractures provide further shear criteria. An asymmetric profile associated with an angle less than 45° (Fig. 13) is characteristic of a transpressive bridge, the shortening being restricted around the small segment. An asymmetric profile combined with an angle of 45–90° defines a tensile bridge (Fig. 13), the short segment corresponding to open fractures or normal faults.

(4) The comparison between models and large-scale field examples indicates that secondary fault segments in compressive bridges are narrower than the adjacent first-generation échelon segments, whereas tensile bridge segments are wider (Fig. 13).

*Acknowledgements*—I gratefully acknowledge Dr S. H. Treagus, Dr P. L. Hancock and an anonymous referee for their suggestions and precise comments, and also Professor W. D. Means who kindly advised me on improvements to this paper.

## REFERENCES

- Bartlett, W. L., Friedman, M. & Logan, J. M. 1981. Experimental folding and faulting of rocks under confining pressure. Part IX. Wrench faults in limestone layers. *Tectonophysics* **79**, 255–278.
- Beach, A. 1975. The geometry of en-échelon vein arrays. *Tectonophysics* **28**, 245–263.
- Clayton, L. 1966. Tectonic depression along the Hope fault, a transcurrent fault in North Canterbury, New Zealand. *N.Z. J. Geol. Geophys.* **9**, 95–104.
- Crowell, J. C. 1974. Sedimentation along the San Andreas Fault. In: *Modern and Ancient Geosynclinal Sedimentation* (edited by Dott, R. H.). *Spec. Publs Soc. econ. Paleontol. Miner., Tulsa* **19**, 292–303.
- Freund, R., Garfunkel, Z., Zak, I., Goldberg, M., Weissbrod, T. & Derrin, B. 1970. The shear along the Dead Sea Rift. *Phil. Trans. R. Soc. A* **267**, 107–130.
- Gamond, J. F. 1983. Displacement features associated with fault zones: a comparison between observed examples and experimental models. *J. Struct. Geol.* **5**, 33–45.
- Gamond, J. F. 1985. Conditions de formation des zones de discontinuités cinématiques dans la croûte supérieure. Aspects expérimentaux et naturels. Unpublished thèse Doctorat, University of Grenoble.
- Gamond, J. F. & Giraud, A. 1982. Identification des zones de faille à l'aide des associations de fractures de second ordre. *Bull. Soc. géol. Fr.*, 7 ser. **XXIV**, 755–762.
- Garfunkel, Z., Zak, I. & Freund, R. 1981. Active faulting in the Dead Sea rift. *Tectonophysics* **80**, 1–26.
- Hancock, P. L. 1972. The analysis of en-échelon veins. *Geol. Mag.* **109**, 269–276.
- Hancock, P. L. 1985. Brittle microtectonics: principles and practice. *J. Struct. Geol.* **7**, 437–457.
- Hancock, P. L. & Atiya, M. S. 1979. Tectonic significance of mesofracture systems associated with the Lebanese segment of the Dead Sea fault. *J. Struct. Geol.* **1**, 143–153.
- Harland, W. B. 1971. Tectonic transpression in Caledonian Spitzbergen. *Geol. Mag.* **108**, 27–42.
- Hempton, M. R. & Neher, K. 1986. Experimental fracture, strain and subsidence patterns over en-échelon strike-slip faults: implications for the structural evolution of pull-apart basins. *J. Struct. Geol.* **8**, 597–605.
- Morgenstern, N. R. & Tchalenko, J. S. 1967. Microscopic structures in kaolin subjected to direct shear. *Geotechnique* **17**, 309–328.
- Naylor, M. A., Mandl, G. & Sijpesteijn, C. H. K. 1986. Fault geometries in basement-induced wrench faulting under different initial stress states. *J. Struct. Geol.* **7**, 737–752.
- Petit, J. P. 1976. La zone de décrochement du Tizi N'Test et son fonctionnement depuis le carbonifère. Unpublished thèse 3ème cycle, Montpellier.
- Petit, J. P., Proust, F. & Tapponnier, P. 1983. Critères de sens de mouvement sur les miroirs de failles en roches non calcaires. *Bull. Soc. géol. Fr.*, 7 ser. **XXV**, 589–608.
- Raynaud, S. 1979. la rupture fragile du granite de la borne (Cévennes) de l'échelle du massif à l'échelle du minéral. Unpublished thèse 3ème cycle, University of Montpellier.
- Robert, J. P. & Vialon, P. 1976. Déformation interne et déformation aux limites dans un assemblage de blocs découpés par un cisaillement. Le clivage schisteux des niveaux structuraux supérieurs. *Bull. Soc. géol. Fr.*, 7 ser. **XVIII**, 1599–1604.
- Sanderson, D. J. & Marchini, W. R. D. 1984. Transpression. *J. Struct. Geol.* **6**, 449–458.
- Segall, P. & Pollard, D. D. 1980. Mechanics of discontinuous faults. *J. geophys. Res.* **85**, 4337–4350.
- Sibson, R. H. 1986. Earthquakes and lineament infrastructure. *Phil. Trans. R. Soc. Lond.* **317**, 63–79.
- Tchalenko, J. S. & Ambraseys, N. N. 1970. Structural analysis of the Dasht-e-Bayaz (Iran) earthquake fractures. *Bull. geol. Soc. Am.* **81**, 41–59.
- Woodcock, N. H. & Fischer, M. 1986. Strike-slip duplexes. *J. Struct. Geol.* **7**, 725–735.
- Xiahoan, L. 1983. Perturbations de contraintes liées aux structures cassantes dans les calcaires fins du Languedoc. Observations et simulations mathématiques. Unpublished thèse 3ème cycle, University of Montpellier.